Korean J. Chem. Eng., 38(6), 1240-1247 (2021)
DOI: 10.1007/s11814-021-0776-6

pISSN: 0256-1115
eISSN: 1975-7220

The role of contact time and input amount of 1,1,1,2-tetrafluoroethane (HFC-134a) on the catalyst lifetime and product selectivity in catalytic pyrolysis

Ali Anus*,‡, Mahshab Sheraz*,‡, Sangjae Jeong, Caroline Mercy Andrew Swamidoss***, Young-Min Kim****, Muhammad Awais Aslam*****, Eui-kun Kim******, and Seungdo Kim*,†**

*Department of Environmental Sciences and Biotechnology, Hallym University, Chuncheon 24252, Korea
**Department of Energy & Environmental Engineering, College of Engineering, Soonchunhyang University, Asan, Chungcheongnam-do 31538, Korea
***Department of Chemistry, Dr. M.G.R. Educational and Research Institute, Chennai, 600095, India
****Department of Environmental Engineering, Daegu University, Gyeongsan 38453, Korea
*****Research Center for Climate Change and Energy, Hallym University, Chuncheon 24252, Korea
******Environment Strategy Development Institute, Hallym University, Chuncheon 24252, Korea
(*Received 9 November 2020 • Revised 20 February 2021 • Accepted 2 March 2021*)

Abstract−During catalytic pyrolysis of HFC-134a over γ-alumina, the formation of HF and coke causes catalyst deactivation. Catalyst deactivation and product selectivity depend on the contact time during catalytic pyrolysis of HFC-134a as reported in this paper. γ-Alumina calcined at 650 °C was used as the catalyst due to its higher quantity of acidic sites and larger surface area, which are crucial for catalytic pyrolysis. X-ray diffraction (XRD), scanning electron microscope-energy dispersive X-ray spectroscopy (SEM-EDS), and thermogravimetric analysis (TGA) of the catalysts were performed to determine the influence of contact time and flow rate of HFC-134a. 2 mL/min of HFC-134a balanced with nitrogen to 25, 50, 100, and 200 mL/min total flow rates was studied at 600 °C. 200 mL/min showed a 9.4 h catalyst lifetime with a small number of by-products. Shorter contact time between HFC-134a and HF with the catalyst was found to be the key to the longer lifetime of the catalyst. The catalyst lifetime was decreased with an increase in the HFC-134a input amount. Among 2, 4, and 6 mL/min input of HFC-134a, 2 mL/min showed the longest catalytic activity followed by 4 and 6 mL/min, respectively. Conversion of γ-alumina into AlF_3 and deposition of coke were responsible for the deactivation.

Keywords: Catalytic Conversion, Pyrolysis, Contact Time, γ-Al_2O_3, HFC-134a

INTRODUCTION

The global temperature has increased rapidly in this past century. Scientists around the world have started taking action in an attempt to solve the issue of global warming, leading to thousands of publications in that arena. Most of these studies conclude that the anthropogenic activities, which laid the foundation of the modern world, are the reason behind this catastrophe [1,2]. Increasing greenhouse gas (GHG) concentrations are considered to have more than 50 percent share in elevation of the global average surface temperature of the earth [3]. Among these GHGs, hydrofluorocarbons (HFCs) are a group of fluorine containing greenhouse gases [4,5] which replaced chlorofluorocarbons (CFCs) and hydrochlorofluorocarbons (HCFCs). CFCs were found to be ozone-depleting substances as they generate chlorine atom by photodissociation which can react with ozone present in the stratosphere [6]. The phasing out of production and consumption of CFCs as a result of the Montreal Protocol [7] resulted in the usage of HFCs as a substitute for refrigerants [5]. Among these HFCs, 1,1,1,2-tetrafluoroethane (HFC-134a) first appeared in the early 1990s as a substitute for the ozone-depleting dichlorofluoromethane ($CHCl_2F$; HCFC-21). It is one of the most abundant HFCs with a global warming potential (GWP) of 1,300 [8]. The emissions of HFCs skyrocketed due to the worldwide increase in the demand for air conditioning. The rising concentration led HFCs to the inclusion in the seven targeted GHGs by the Kyoto Protocol [4]. In 2016, the Kigali Amendment to the Montreal Protocol decided to phase down the consumption of HFCs, eager to avoid emission of 70 billion tons CO_2 equivalent (CO_2e) by 2050 [9]. Therefore, technologies for the climate change mitigation caused by HFCs, especially HFC-134a, are of tremendous importance.

At present, the treatment methods of HFC-134a majorly include thermal combustion, plasma decomposition, and catalytic decomposition. Thermal combustion is considered to be the most applicable technology for the decomposition of HFCs and Perfluorocarbons (PFCs) so far. It is also certified by the United Nations Framework on Climate Change (UNFCC) to abate HFC-23 under clean development project [10], as it is the highly efficient and simplest treatment method for the HFCs disposal. However, being that fuel is required for this process, commercialization is difficult. It is also not easy to obtain inexpensive material for the reaction

†To whom correspondence should be addressed.
E-mail: sdkim@hallym.ac.kr
‡These authors contributed equally to this work.
Copyright by The Korean Institute of Chemical Engineers.

compartment. The compulsory post-treatment is yet another unfortunate hindrance due to the formation of toxic by-products, such as dioxins, corrosive acids, NOx, etc. [11,12].

Plasma technology is also growing rapidly in the field of decomposition of fluorinated compounds. Fascinating results in the literature suggest high decomposition (up to 99.9%) is possible [13]. Moreover, unwanted byproducts like COF_2 are also reported to be controlled and it is considered proficient for HFC-134a treatment over a wide range of initial concentrations [14,15]. Even so, this technology is expensive and less energy efficient, which causes restraints in its dominance [12].

For the decomposition of HFCs and other fluorinated compounds including PFCs, NF_3, SF_6, catalytic pyrolysis was proven to be a safe, more practical, and convenient method as it requires a comparatively lower temperature than other techniques, which makes this method cost-effective as well [16,17]. Nearly 100% HFC-134a was destructed at 600 °C when concrete waste was employed as a catalyst [18]. Metal phosphates were also studied as the catalysts and promising results strengthened the concept of catalytic pyrolysis when the conversion reached 100% at only 500 ° without any hazardous byproducts [16].

In the search of a more economical path, the catalytic activity of five catalysts was studied. γ-Alumina was reported to have the highest activity among the used catalysts [19]. The catalytic activity of γ-alumina is supported by other studies on catalytic pyrolysis as well [20,21]. The alumina catalyst rapidly deactivates due to its conversion to AlF_3 [19]. To increase the stability of alumina catalysts, metal-doped alumina based catalysts were studied in which Ce [22], Ni [23], and Mg [24] are some of the reported metals which perceived catalyst lifetime when introduced in alumina and convert HFC-134a into trifluoroethylene (C_2HF_3, TrFE). Trifluoroethylene is an important organic molecule used as a precursor for fluoro-plastics and fluoro-rubber [25], co-monomer [26] as well as future refrigerant due to its low GWP [27].

So far, there is no study available which shows the significance of contact time in catalytic decomposition of HFC-134a, which is a very important step for gas phase reactions. Therefore, this article is focused on the catalytic pyrolysis of HFC-134a at various space velocities, in other words, the contact time of HFC-134a over γ-alumina. Our goal was to determine which space velocity or contact time is responsible to get the least number of products to achieve highly pure trifluoroethylene by the catalytic decomposition of HFC-134a. Also, how it will have an effect on catalyst lifetime as higher space velocity will lower the possibility of the gas-solid reaction and HF-attack on the catalyst. Different flow rates of input gases were used to select the best achievable conditions for our goal. XRD, TGA, and SEM-EDS were used to identify the changes in the catalyst. To determine the conversion rate, GC/MS was used to study the samples of the product gas.

MATERIALS AND METHODS

1. Raw Materials

γ-Alumina was purchased from Alfa Aesar (USA). The γ-alumina was employed after calcining for 2 h at 650 °C in the air. After the calcination, the catalyst was crushed and then sieved to extract particle size between 1.0-1.7 mm. The surface area of the fresh catalyst was found to be 187 m^2/g. The acidic sites were also studied for the fresh catalyst. The amount of weak, intermediate, and strong acidic sites was quantified as 1.776, 2.345, and 2.623 mmol-NH_3/g-catalysts, respectively. HFC-134a was acquired from RIGAS Co. Ltd. (Korea). CaO was purchased from Junsei Chemicals (Japan).

2. Experiment Details

A decomposition study of HFC-134a was done at 600 °C using a plug flow reactor made with an SUS-316L tube loaded with alu-

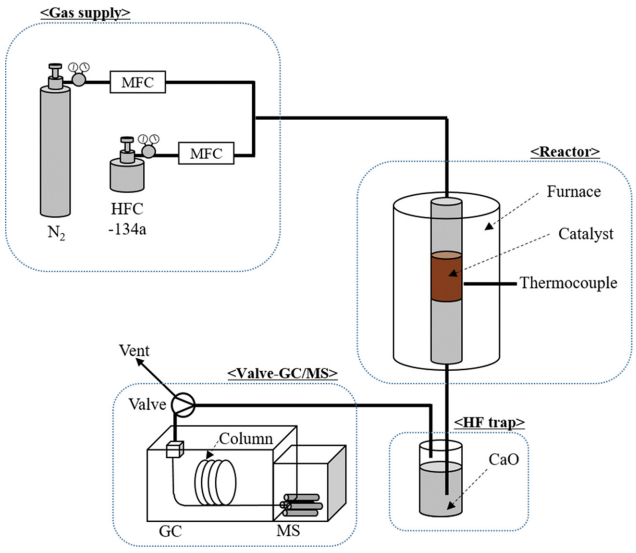


Fig. 1. Schematic diagram of the pyrolysis system used for the studies [24].

Table 1. Contact time and GHSV at used flow rates

Total flow rate (mL/min)	Mixing amount (HFC+N_2)	Contact Time = $\frac{\text{Volume of catalyst} \times 60}{\text{Flow rate}}$ (s)	GHSV = $\frac{\text{Flow rate} \times 60}{\text{Catalyst weight}}$ ($mL g^{-1}_{cat} h^{-1}$)
25	2+23	8.64	1,250
50	2+48	4.32	2,500
100	2+98	2.16	5,000
200	2+198 4+196 6+194	1.08	10,000

mina catalyst connected to the GC/MS. The setup of the pyrolysis system is shown in Fig. 1. The amount of alumina catalyst used in the reactor was 1.2 g, whereas the flow rate of 2, 4, and 6 mL/min of HFC-134a was introduced in the reactions. Nitrogen was used to maintain the required total flow rate of 25, 50, 100, and 200 mL/min. Table 1 shows the different total flow rates used in this study as well as HFC-134a and N_2 proportions. Mass flow controllers (Kofloc, Kojima Instruments Inc.) were used to control the gas flow. A thermocouple was used to monitor the reaction temperature. CaO was used to capture the HF produced after the pyrolysis before sending the sample to GCMS for analysis.

The sample was analyzed by using Shimadzu GC/MS (QP2020) equipped with GS-GASPRO column, National Institute of Standards and Technology (NIST) MS library was used to identify the peaks in MS chromatogram, and GCMSsolution used to study peaks and calculate the peak area. To determine the conversion rate, calculated peak areas of input and output gas were applied in Eq. (1).

$$\text{Conversion (\%)}=(1-A_{out}/A_{in})\times 100 \quad (1)$$

where A_{in} denotes the peak area of input gas (HFC-134a) and product gas is mentioned as A_{out}.

3. Characterization

The catalyst phase was identified by high-resolution X-Ray diffractometer (model: D/Max-2500V, Rigaku) within the 2θ scan range of 10-80°. Field emission scanning electron microscope/energy dispersive spectrometer (model: JSM-6701F/X-Max, Jeol) was practiced to examine the morphology, texture, and chemical composition of the catalyst surface. The coke content was analyzed by thermogravimetric analyzer (model: TGA55, TA Instruments).

RESULTS AND DISCUSSION

1. Effect of Contact Time on Catalyst Lifetime

The main reaction by which HFC-134a is decomposed is an elimination reaction as shown in Eq. (2) where it breaks into trifluoroethylene and hydrofluoric acid (HF). The contact time was controlled by the total flow rate of HFC-134a, which was the reactant gas and nitrogen which was used as balance gas. Fig. 2 shows the decomposition tendency of HFC-134a by using 1.2 g γ-alumina as the catalyst at 600 °C with 2 mL/min HFC-134a balanced by nitrogen to the total flow rates of 25, 50, 100, and 200 mL/min. The contact time and gas hourly space velocity at different flow rates are given in Table 1. There is an inverse relationship between contact time and flow rate because the contact time decreases with an increase in the flow rate. The conversion of HFC-134a was more than 95% at all the contact times at the initial stage. But the stability of the catalyst was highly affected. The shortest contact time is at 200 mL/min, maintained the conversion for the longest time and the catalyst lifetime decreased with the increase in contact time. The catalyst lifetime in this study is considered as the time when the conversion was decreased to 95%. It was observed that the catalyst lifetime increased from around 1 h with 25 mL/min flow rate to 9.4 h at 200 mL/h total flow.

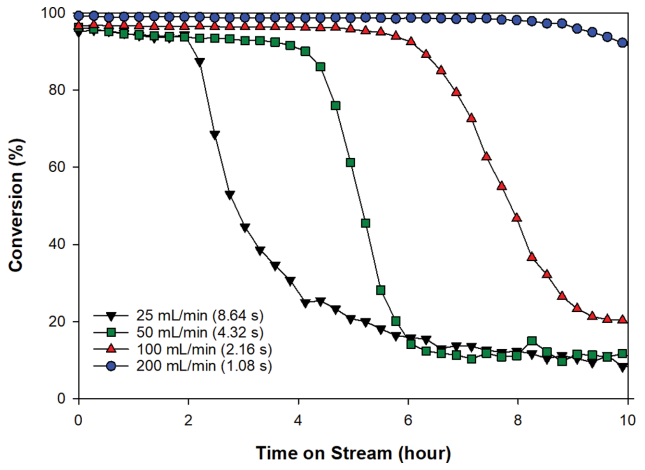


Fig. 2. Conversion of HFC-134a at different total flow rate at 600 °C.

Yaghobi stated that generally high space velocity is recommended for the catalytic process if it does not decrease catalyst lifetime and conversion [28]. Açıkalın et al. stated that residence time (contact time) is an important factor in pyrolysis as it effects the gas-solid reaction [29]. This means by increasing the flow rate of input gas, the contact time of formed HF and HFC-134a itself with the catalyst becomes short. HF and HFC-134a can react with alumina and convert it into aluminum fluoride, which can deactivate the catalyst as shown in Eq. (3) and (4). So, with a higher flow rate deactivation of catalyst delays.

$$CH_2FCF_3 \rightarrow CHF=CF_2+HF \quad (2)$$

$$CH_2FCF_3+Al_2O_3 \rightarrow\rightarrow C+CO_2+H_2O+HF+AlF_3 \quad (3)$$

$$6HF+Al_2O_3 \rightarrow 2AlF_3+3H_2O \quad (4)$$

2. Effect of Contact Time on Product Selectivity

The relative amount of products was found by calculating the ratio between the peak areas of products and peak area of input HFC-134a ,which can be seen in Fig. 3. Another effect of contact time was observed that at the total flow rate of 25 mL/min (longest contact time), carbon dioxide was formed as a major product in the first hour of the reaction and a very small amount of trifluoroethylene was produced. It suggests that during the first hour, due to longer contact time, HFC-134a was mainly decomposed with gas-solid reaction with alumina catalyst as given in Eq. (3) instead of catalytic elimination of HF (Eq. (2)). It was also interesting to observe that when the catalyst started to deactivate, different byproducts were also detected, including tetrafluoromethane, hexafluoroethane, trifluoromethane, pentafluoroethane, 1,1,1-trifluoroethane, 1,1,2-trifluoroethane with the total flow rate of 25 mL/min. It is assumed that radical reactions are occurring as side reactions at a low total flow rate (long contact time). The same by-products during the catalyst deactivation period were observed with 50 mL/min total flow rate, but trifluoroethylene was found to be the main product with a large amount of carbon dioxide throughout the reaction.

When the total flow rate was set as 100 mL/min and 200 mL/min, only trifluoroethylene and carbon dioxide were found as products and later showed higher trifluoroethylene and lower carbon

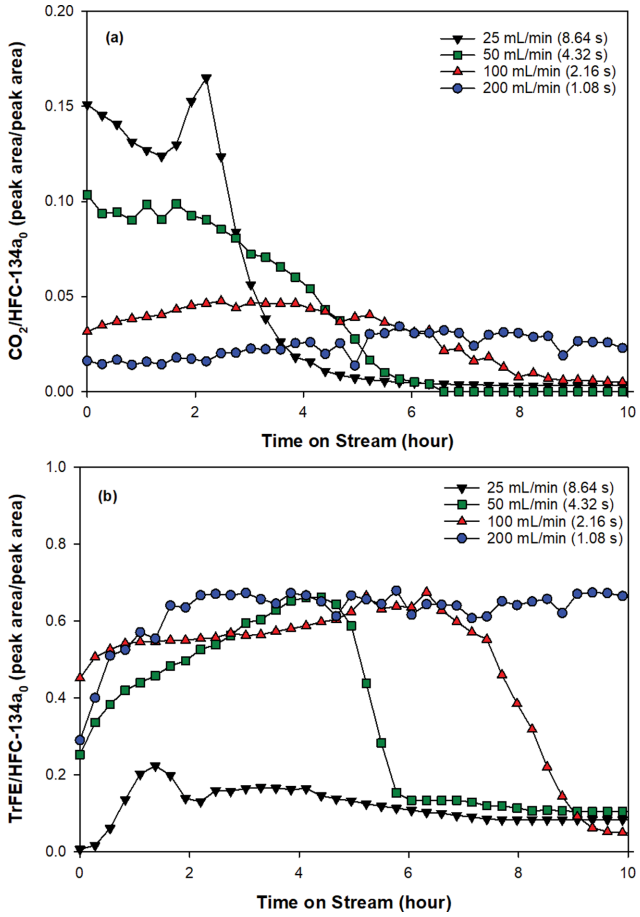
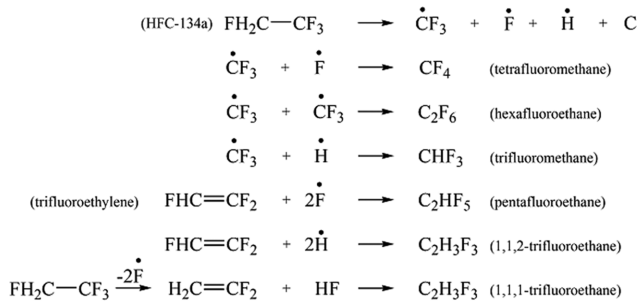


Fig. 3. Formation of products at 600 °C with different total flow rate. (a) CO_2, (b) TrFE.

dioxide. It was observed that carbon dioxide has a direct relation with the contact time as its yield increased with the increase in contact time. In the case of trifluoroethylene, it was clearly seen that its yield was increased with the total flow rate, which means contact time at 100 and 200 mL/min total flow rate is enough for the production of trifluoroethylene but not enough for other products. These results show that the contact time of input gas with the catalyst is very crucial for the selectivity between the elimination of HF and gas-solid reaction. Yang et al. [30] studied the contact time effect on catalytic pyrolysis of cellulose and concluded that contact time of reactant with catalyst had a huge impact on product formation; they also observed that longer contact time leads to the formation of CO_2. Other studies [28,31,32] also stated that product selectivity is dependent on contact time.

According to the literature [29,33], longer contact time causes secondary reactions like repolymerization or thermal cracking or re-condensation. In our studies, the various by-products formed at a lower flow rate can be produced by the above-mentioned reactions. Scheme 1 explains the reaction mechanisms for observed by-products. It was suspected that substantial thermal-cracking of HFC-134a took place at longer contact times. This thermal-cracking was responsible for generating numerous radicals. These radicals recombined and formed different by-products.



Scheme 1. Reaction mechanisms for the by-products.

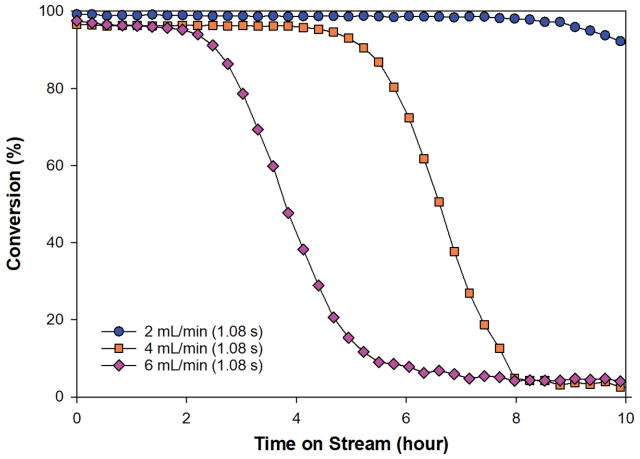


Fig. 4. Conversion at different flow rates of HFC-134a with a total flow of 200 mL/min at 600 °C.

3. HFC-134a Flow Rate

After determining the effect of contact time through the total flow rate, we studied the effect of HFC-134a input. As shown in Fig. 4 the flow rate of HFC-134a used was 2, 4, and 6 mL/min balanced with nitrogen gas to a total flow rate of 200 mL/min, which showed the highest catalyst lifetime and lower number of products. It was observed that the catalyst lifetime decreased with an increase in the input amount of HFC-134a in the reactor. The lifetime of 4 mL/min HFC-134a flow rate was found to be 4.7 h, and for 6 mL/h flow rate the conversion was maintained for 1.9 h and both of them were significantly lower than 2 mL/min (9.4 h). It can be seen that the lifetime of the catalyst depends upon the concentration of input gas. Trifluoroethylene and carbon dioxide were detected as products in both reactions.

Interestingly, in the case of 2 and 4 mL/min HFC-134a flow rate, as the HFC-134a input was doubled, the catalyst lifetime was reduced by half. In this case, the decomposition capacity of the catalyst (HFC-134a flow rate×catalyst lifetime) remained the same for both cases. From this observation, it can be concluded that there is a specific input amount that can result in high decomposition capacity in a short time. This decrease in process time can be environmentally crucial as well as economically beneficial by saving balance gas and energy.

4. Physicochemical Properties of the Catalyst

The results of the XRD analysis of fresh and used catalysts are

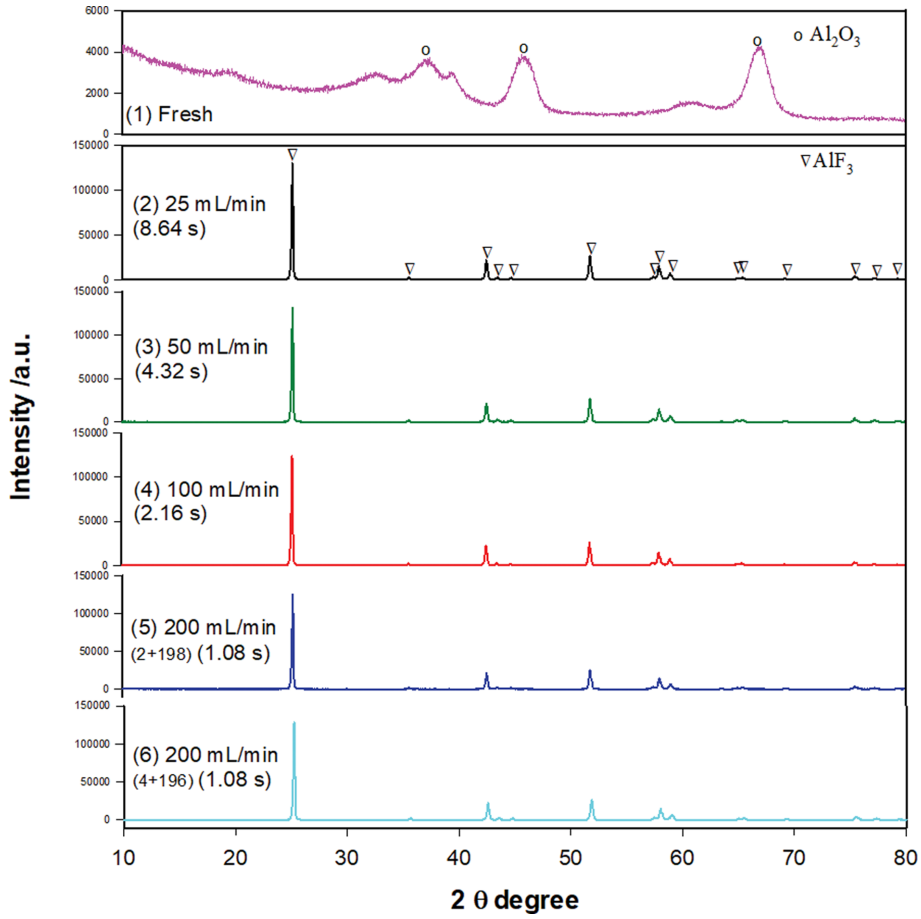


Fig. 5. XRD spectra of fresh and used catalysts.

shown in Fig. 5. Peaks of γ-alumina were found in fresh catalyst calcined at 650 °C, which we also observed in our previous studies [24,34]. In all used catalysts, the peaks of α-AlF_3 (JCPDS: 01-080-1007) were detected with the characteristic peaks at 2θ (hkl) 25° (012), 42° (113), 52° (024), and 58° (116). It was suggested that the conversion of γ-alumina to inactive AlF_3 through reactions explained in Eqs. (3) and (4) is the reason for the loss in the catalytic activity of the catalyst. Peak intensity (area and height) of four major peaks (hkl: 012, 113, 024, and 116) of used catalysts was monitored and added as Table S1 in Supplementary Information to determine the damage to γ-alumina. The catalyst used with 200 mL/min was found to have slightly lower peak intensity than the catalysts used with lower flow rate. It was observed that catalysts were faintly more damaged in a shorter amount of time with lower flow rates; on the other hand, longer time was taken by the catalyst decomposition with higher flow rates. It is suggested that a higher flow rate is decreasing the contact time for HF or HFC-134a to react with γ-alumina, hence slowing the deactivation of the catalyst. Tsenga and Chao [35] also performed a quantitative analysis of anatase and rutile in a sample with the help of XRD intensity on the basis of literature [36]. The researchers stated that the peak intensity of rutile was decreased with the increase in intensity of anatase and vice versa. This change in intensities occurred with the conversion of anatase to rutile as the temperature increased.

Higher peak intensity of AlF_3 was also observed when the HFC-134a input was increased to 4 mL/min. The higher HFC-134a input resulted in a higher amount of HF, which caused fluorination of alumina quicker and deactivation occurred earlier than 2 mL/min flow rate of HFC-134a. 4 mL/min damaged more catalyst than 2 mL/min HFC-134a input in shorter amount of time.

The conversion of γ-alumina into AlF_3 can be reduced by regeneration of the catalyst. Jeon et al. [37] claimed that AlF_3 was not

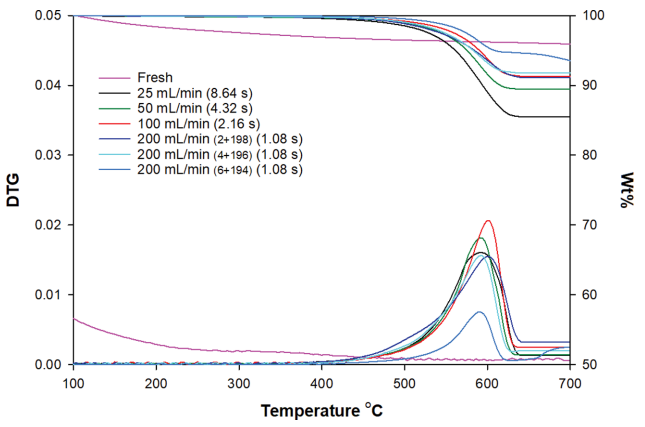


Fig. 6. TGA spectra of fresh and used catalysts.

detected in used catalyst when γ-alumina was impregnated with phosphate for the hydrolytic decomposition of PFCs. They suggested that the catalyst was regenerated under applied conditions and the reaction given in Eq. (4) was moved backwards. On the other hand, Han et al. [19] reported than in the absence of phosphate, AlF_3 was observed in used catalyst after the hydrolytic decomposition of HFC-134a. More studies are required in this field to maximize the catalytic performance of γ-alumina.

Fig. 6 gives the weight loss of the fresh and used catalysts through TGA. The catalyst deactivated quickly at the flow rate of 25 mL/min and the largest coke amount was formed (11.4%±1% wt) followed by 50 mL/min (7.4%±1% wt), 100 mL/min (5.8%±1% wt) and 200 mL/min (6.2%±1% wt). In our previous studies, it was also observed that the catalyst lifetime is linked to the coke amount produced in the course of the reaction to a great extent [24]. This observation strengthens the suggestion given earlier in this paper that the chances of a gas-solid reaction are greater with longer contact time (25 and 50 mL/min) than shorter (100 and 200 mL/min). The high amount of coke, CO_2, and also AlF_3 were observed with longer contact time and all of them were significantly reduced with shorter contact time. This means shorter contact time can be applied to reduce catalyst deactivation through coke formation, which results in a longer lifetime of the catalyst. Among different input amounts of HFC-134a, the coke amount decreases with a

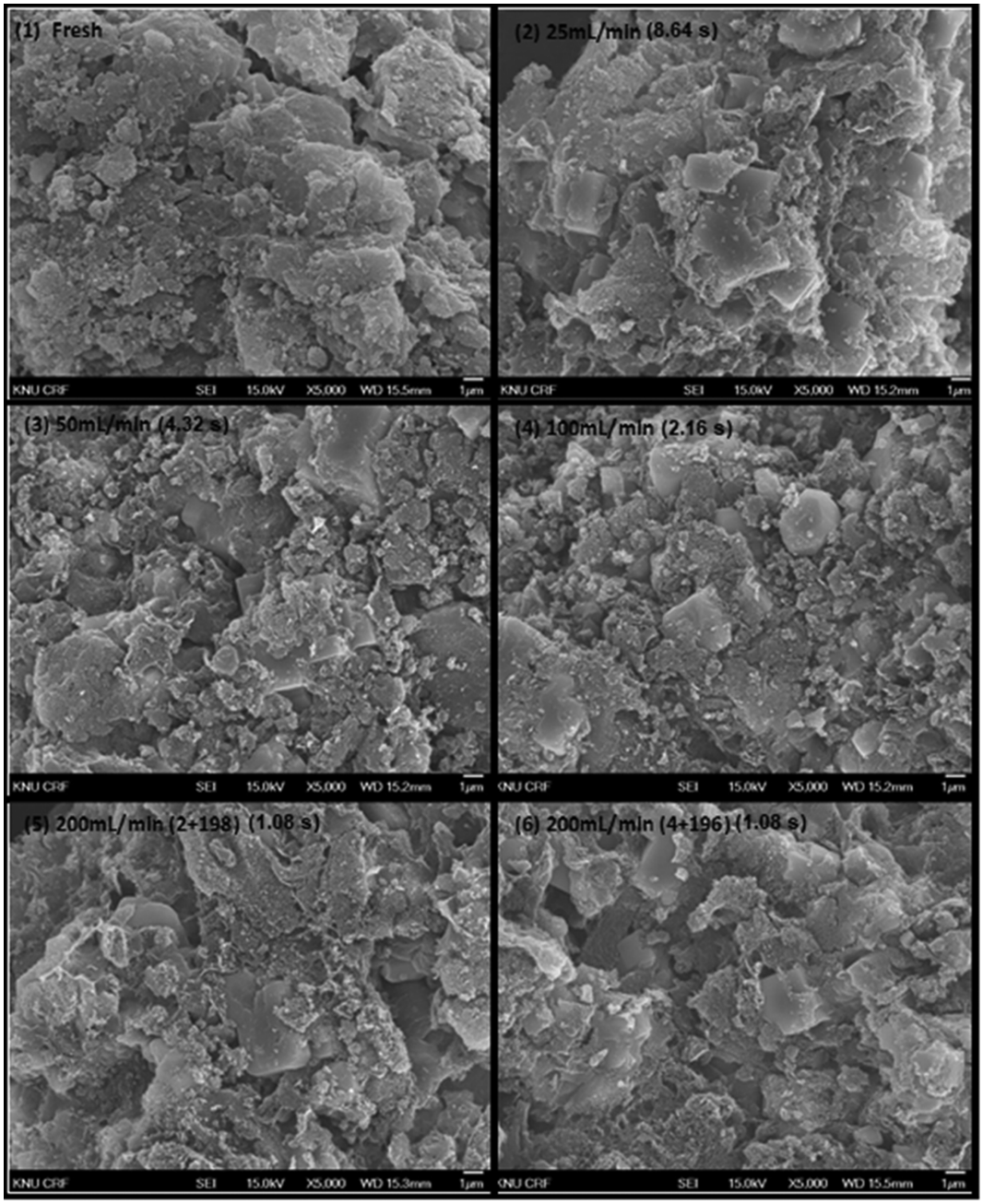


Fig. 7. SEM images of fresh and used catalysts for different flow rates at magnification 5,000×.

Table 2. Elemental composition on the surface of catalysts through EDS

Reaction conditions	γ-Al_2O_3 (element, wt%)				Coke (TGA)
	Al	O	F	C	% wt
Fresh	51.02	48.98	-	-	
25 mL/min (8.64 s)	12.46	-	44.58	42.96	11.4
50 mL/min (4.32 s)	13.69	-	49.44	36.87	7.4
100 mL/min (2.16 s)	14.31	-	53.20	32.49	5.8
200 mL/min (2+198) (1.08 s)	14.10	-	50.50	35.40	6.2
200 mL/min (4+196) (1.08 s)	14.34	-	47.64	38.02	5.5

decrease in catalyst lifetime. This suggests that at shorter contact time, catalyst deactivation occurs mainly due to fluorination of the catalyst and it is independent of the input amount of HFC-134a.

Our previous study [34] observed that a high amount of coke was formed after the deactivation of the catalyst. It was suggested that 25 mL/min flow rate provided a longer contact time for HF to react with γ-alumina to form AlF_3 early in the reaction (Eq. (4)). The gas-solid reaction between HFC-134a and γ-alumina formed CO_2, as shown in Fig. 3(a), is also responsible for the production of AlF_3, as given in Eq. (3). The α-AlF_3 was formed due to catalyst deactivation, which is the strong Lewis acid [38]; there is a possibility that it can also lead to the formation of coke and polymeric by-products [25]. Xi et al. also reported that due to strong Lewis acidic sites, the AlF_3 catalyst produces coke and causes deactivation [39]. On the other hand, with 200 mL/min the formation of AlF_3 is slower, hence lesser amount of coke is observed. It is important to mention that formation of trifluoroethylene by the elimination of HF from HFC-134a is dependent on weak Lewis acidic sites [25].

Fig. 7 shows SEM images of fresh and used catalyst; it is very clear that the morphology of catalyst is changed, which indicates the deactivation of the catalyst. Crystals of AlF_3 are visible in all the used catalyst samples after the reaction due to the conversion of γ-alumina into AlF_3. The crystals of AlF_3 can be seen covered in carbon (coke) produced during the reaction. The elemental composition from the EDS is given in Table 2 with the coke amount determined from TGA. In fresh catalyst, Al and O were the only elements detected in EDS. Whereas in the used catalysts, F, C, and Al were detected but O was absent from all the samples. It was interesting to see that, like TGA, the catalyst used with 25 mL/min flow rate showed a larger amount of coke in EDS after a shorter catalytic lifetime than 200 mL/min. The distribution of atoms can be seen in Fig. S1 in supplementary information. Al and O atoms are evenly dispersed on the surface of the fresh catalyst. Sporadic dispersion of atoms was found on the surface of the spent catalyst. Some surfaces have a higher concentration of C where others have higher Al and F. AlF_3 was also found on the surface of the used catalysts when Ga doped γ-Al_2O_3 with and without the pretreatment of sulfuric acid was used for the hydrolytic decomposition of HFC-134a [40].

CONCLUSION

This study focused on the effect of the contact time of the input gas mixture by controlling the total flow rate as well as the input amount of HFC-134a on the catalyst lifetime and the selectivity of the product in the catalytic pyrolysis. Among the different investigated total flow rates with 2 mL/min HFC-134a, 200 mL/min showed the longest lifetime and least number of by-products while having the lowest contact time. Shorter contact time delays catalyst deactivation. The shorter contact time minimizes the reaction of HF and HFC-134a with the catalyst as well as the decomposition of HFC-134a through the radical mechanism. When the input amount of HFC-134a was increased, no change in product selectivity was observed. The catalyst lifetime decreased with the increase in the HFC-134a amount. 2 mL/min flow rate of HFC-134a was found to maintain the conversion for longer than 4 and 6 mL/min. TGA, XRD, and SEM-EDS of the used and fresh catalysts were performed. It was concluded that the drop in catalyst lifetime was observed due to the deactivation of the catalyst. γ-Alumina can be converted to AlF_3 by reacting with HF formed during the decomposition. It was also stated that coke formation due to gas-solid reaction between HFC-134a and γ-alumina is also responsible for catalyst deactivation.

ACKNOWLEDGEMENT

This research was supported by a grant (20UGCP-B157945-01) from the Urban-based complex plant demonstration study utilizing underground space program funded by the Ministry of Land, Infrastructure, and Transport, Republic of Korea, and by Basic Science Research Program through the National Research Foundation of Korea (NRF) funded by the Ministry of Education (grant number) (NRF-2019R1A6A3A01096378).

CONFLICT OF INTEREST

The authors declare no conflict of interest.

SUPPORTING INFORMATION

Additional information as noted in the text. This information is available via the Internet at http://www.springer.com/chemistry/journal/11814.

REFERENCES

1. D. J. Wuebbles, D. R. Easterling, K. Hayhoe, T. Knutson, R. E. Kopp,

J. P. Kossin, K. E. Kunkel, A. N. LeGran-de, C. Mears, W. V. Sweet, P. C. Taylor, R. S. Vose and M. F. Wehner, 2017: Our globally changing climate. In: Climate Science Special Report: Fourth National Climate Assessment, Volume I [Wuebbles, D. J., D. W. Fahey, K. A. Hibbard, D. J. Dokken, B. C. Stewart and T. K. Maycock (eds.)]. U.S. Global Change Research Program, Washington, DC, USA, pp. 35-72.
2. J. Srinivasan, *Resonance*, **13**(12), 1146 (2008).
3. IPCC, 2014: Climate Change 2014: Synthesis Report. Contribution of Working Groups I, II and III to the Fifth Assessment Report of the Intergovernmental Panel on Climate Change [Core Writing Team, R. K. Pachauri and L. A. Meyer (eds.)]. IPCC, Geneva, Switzerland, 151 pp.
4. https://ec.europa.eu/clima/policies/strategies/progress/kyoto_2_en (accessed Sep. 21, 2020).
5. G. J. M. Velders, A. R. Ravishankara, M. K. Miller, M. J. Molina, J. Alcamo, J. S. Daniel, D. W. Fahey, S. A. Montzka and S. Reimann, *Science*, **335**(6071), 922 (2012).
6. M. J. Molina and F. S. Rowland, *Nature*, **249**, 810 (1974).
7. https://ozone.unep.org/treaties/montreal-protocol (accessed Oct. 07, 2020).
8. G. Myhre, D. Shindell, F.-M. Bréon, W. Collins, J. Fuglestvedt, J. Huang, D. Koch, J.-F. Lamarque, D. Lee, B. Mendoza, T. Nakajima, A. Robock, G. Stephens, T. Takemura and H. Zhang, 2013: Anthropogenic and Natural Radiative Forcing. In: Climate Change 2013: The Physical Science Basis. Contribution of Working Group I to the Fifth Assessment Report of the Intergovernmental Panel on Climate Change [Stocker, T. F., D. Qin, G.-K. Plattner, M. Tignor, S. K. Allen, J. Boschung, A. Nauels, Y. Xia, V. Bex and P. M. Midgley (eds.)]. Cambridge University Press, Cambridge, United Kingdom and New York, NY, USA.
9. https://eia-international.org/wp-content/uploads/EIA-Kigali-Amendment-to-the-Montreal-Protocol-FINAL.pdf (accessed Oct. 28, 2020).
10. UNFCCC, *CDM Methodology Booklet*, 2019.
11. M. Shin, D. Jang, Y. Lee, Y. Kim and E. Kim, *J. Mater. Cycles Waste Manag.*, **19**(2), 754 (2017).
12. W. Han, Y. Li, H. Tang and H. Liu, *J. Fluorine Chem.*, **140**, 7 (2012).
13. M. Ohno, Y. Ozawa and T. Ono, *Int. J. Plasma Environ. Sci. Technol.*, **1**(2), 159 (2007).
14. M. S. Gandhi and Y. S. Mok, *Int. J. Environ. Sci. Technol.*, **12**(2), 499 (2013).
15. Y. F. Wang, W. J. Lee, C. Y. Chen and L. Te Hsieh, *Ind. Eng. Chem. Res.*, **38**(9), 3199 (1999).
16. Y. Takita, T. Tanabe, M. Ito, M. Ogura, T. Muraya, S. Yasuda, H. Nishiguchi and T. Ishihara, *Ind. Eng. Chem. Res.*, **41**(11), 2585 (2002).
17. Z. M. El-Bahy, R. Ohnishi and M. Ichikawa, *Appl. Catal. B Environ.*, **40**(2), 81 (2003).
18. A. Iizuka, H. Ishizaki, A. Mizukoshi, M. Noguchi, A. Yamasaki and Y. Yanagisawa, *Ind. Eng. Chem. Res.*, **50**(21), 11808 (2011).
19. T. U. Han, B. Yoo, Y. Kim, B. Hwang, G. L. Sudibiya, Y. Park and S. Kim, *Korean J. Chem. Eng.*, **35**(8), 1611 (2018).
20. X. F. Xu, J. Y. Jeon, M. H. Choi, H. Y. Kim, W. C. Choi and Y. K. Park, *J. Mol. Catal. A Chem.*, **266**(1-2), 131 (2007).
21. W. Han, Y. Chen, B. Jin, H. Liu and H. Yu, *Greenh. Gases Sci. Technol.*, **4**(1), 121 (2014).
22. J. Song, S. Chung, M. Kim, Y. Lee, K, Lee and J. Kim, *J. Mol. Catal. A Chem.*, **370**, 50 (2013).
23. W. Jia, M. Liu, X. Lang, C. Hu, J. Li and Z. Zhu, *Catal. Sci. Technol.*, **5**(6), 3103 (2015).
24. C. M. A. Swamidos, M. Sheraz, A. Anus, S. J. Jeong, Y. Park, Y. Kim and S. Kim, *Catalysts*, **9**(3), 270 (2019).
25. W. Jia, Q. Wu, X. Lang, C. Hu, G. Zhao, J. Li and Z. Zhu, *Catal. Lett.*, **145**(2), 654 (2015).
26. J. Ryu, K. No, Y. Kim, E. Park and S. Hong, *Sci. Rep.*, **6**, 36176 (2016).
27. Y. Higashi, N. Sakoda, M. A. Islam, Y. Takata, S. Koyama and R. Akasaka, *J. Chem. Eng. Data*, **63**(2), 417 (2018).
28. N. Yaghobi, *J. King Saud Univ. - Eng. Sci.*, **25**(1), 1 (2013).
29. K. Açikalin, F. Karaca and E. Bolat, *Fuel*, **95**, 169 (2012).
30. H. Yang, R. Coolman, P. Karanjkar, H. Wang, P. Dornath, H. Chen, W. Fan, W. C. Conner, T. j. Mountziaris, and G. Huber, *Green Chem.*, **19**(1), 286 (2017).
31. H. Y. Li, Y. J. Yan and Z. W. Ren, *J. Fuel Chem. Technol.*, **36**(6), 666 (2008).
32. A. Aho, A. Tokarev, P. Backman, N. Kumar, K. Eränen, M. Hupa, B. Holmbom, T. Salmi and D. Y. Murzin, *Top. Catal.*, **54**, 941 (2011).
33. E. Pütün, *Energy*, **35**(7), 2761 (2010).
34. S. J. Jeong, G. L. Sudibya, J. Jeon, Y. Kim, C. M. A. Swamidoss and S. Kim, *Catalysts*, **9**(11), 901 (2019).
35. W. J. Tseng and P. S. Chao, *Ceram. Int.*, **39**, 3779 (2013).
36. R. A. Spurr and H. Myers, *Anal. Chem.*, **29**, 760, (1957).
37. J. Y. Jeon, X.-F. Xu, M. H. Choi, H. Y. Kim and Y.-K. Park, *Chem. Commun.*, **3**, 1244 (2003).
38. T. Krahl and E. Kemnitz, *Catal. Sci. Technol.*, **7**(4), 773 (2017).
39. Z. Xi, X. Liu, J. Li, J. Yuan, W. Jia, X. Liu, M. Liu and Z. Zhu, *ChemistrySelect*, **4**(15), 4506 (2019).
40. M. Kim, Y. Kim, J. Youn, I. Choi, K. Hwang, S. G. Kim, Y. Park, S. Moon, K. B. Lee and S. Jeon, *Catalysts*, **10**(7), 766 (2020).

Supporting Information

The role of contact time and input amount of 1,1,1,2-tetrafluoroethane (HFC-134a) on the catalyst lifetime and product selectivity in catalytic pyrolysis

Ali Anus[*,‡], Mahshab Sheraz[*,‡], Sangjae Jeong[**], Caroline Mercy Andrew Swamidoss[***], Young-Min Kim[****], Muhammad Awais Aslam[*****], Eui-kun Kim[******], and Seungdo Kim[*,†]

*Department of Environmental Sciences and Biotechnology, Hallym University, Chuncheon 24252, Korea
**Department of Energy & Environmental Engineering, College of Engineering, Soonchunhyang University, Asan, Chungcheongnam-do 31538, Korea
***Department of Chemistry, Dr. M.G.R. Educational and Research Institute, Chennai, 600095, India
****Department of Environmental Engineering, Daegu University, Gyeongsan 38453, Korea
*****Research Center for Climate Change and Energy, Hallym University, Chuncheon 24252, Korea
******Environment Strategy Development Institute, Hallym University, Chuncheon 24252, Korea
(*Received 9 November 2020 • Revised 20 February 2021 • Accepted 2 March 2021*)

Table S1. Peak areas and intensities of major AlF_3 peaks in used catalyst for 2 mL/min HFC-134a flow rate

hkl	25 mL/min (8.64 s)		50 mL/min (4.32 s)		100 mL/min (2.16 s)		200 mL/min (1.08 s)	
	Intensity	Peak Area	Intensity	Peak Area	Intensity	Peak Area	Intensity	Peak Area
012	97,196	1,656,706	97,517	1,665,401	93,043	1,577,239	94,995	1,561,473
113	16,932	385,244	17,073	384,555	17,534	379,387	16,854	359,151
024	21,999	490,590	22,386	490,855	21,654	472,312	21,008	455,138
116	12,562	349,967	12,381	326,670	12,531	311,961	12,140	298,338

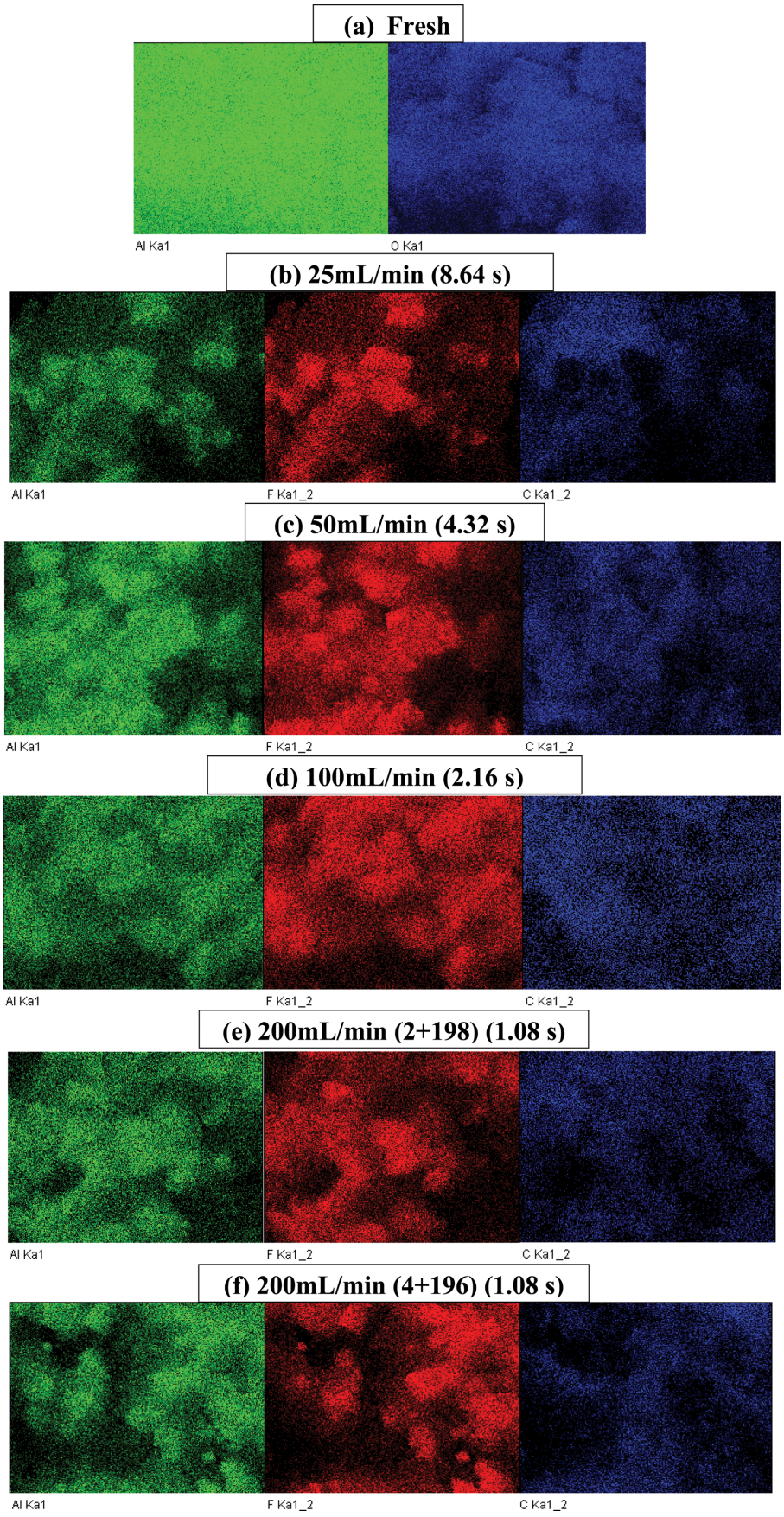


Fig. S1. EDS image of fresh and spent catalysts.